CHINESE JOURNAL OF PHYSICS VOL. 52, NO. 1-II February 2014

Review

Effect of Ionization on the Wavelength Scaling of High Harmonic Generation Efficiency

Jun Dai, Zhinan Zeng,* Candong Liu, Ruxin Li,† and Zhizhan Xu‡

State Key Laboratory of High Field Laser Physics,
Shanghai Institute of Optics and Fine Mechanics,
Chinese Academy of Sciences, Shanghai 201800, China
(Received August 30, 2013)

The physical origin of the recently reported wavelength scaling law of high harmonics generation (HHG) yield [Tate *et al.*, Phys. Rev. Lett. 98, 013901 (2007); Shiner *et al.*, Phys. Rev. Lett. 103, 073902 (2009)] is not fully understood. We re-investigate theoretically the wavelength (from 800 nm to 2000 nm) scaling of HHG yield in atoms with different soft-core Coulomb potentials. It is found that the power x of the wavelength scaling λ^x surprisingly oscillates in the region $-3.63 \sim -6.32$. A similar oscillation is found in the wavelength scaling of ionization ratio upon the ionization potential, indicating that the wavelength scaling of HHG yield is closely relevant to the ionization. The origin of this oscillation in ionization is also identified.

DOI: 10.6122/CJP.52.320 PACS numbers: 42.65.Ky, 32.80.Rm, 32.80.Fb

HHG in atoms and molecules is a primary approach for table-top coherent sources in the extreme ultraviolet (XUV) region. To pursue a shorter wavelength emission, a longer wavelength laser driver is desirable according to the well-known cutoff law of HHG, i.e. the highest photon energy is approximately $I_p + 3.17U_p$ [1, 2], where I_p denotes the ionization potential of the target atom, $U_p = F_0^2/4\omega^2$ is the ponderomotive energy, F_0 is the peak electric field and ω is the angular frequency. A longer wavelength pulse can push the cutoff to higher photon energy, since U_p increases quadratically with the wavelength λ. This wavelength scaling law and the favorable phase matching conditions motivated the HHG experiments using intense mid-infrared laser pulses [3–6] and the water-window HHG have been demonstrated recently by several groups [7–9].

The major concern in the HHG driven by longer wavelength laser pulses is the efficiency. It has been commonly assumed that the wavelength scaling of HHG yield is λ^{-3} [10]. However, a more rapid decrease in HHG yield as $\lambda^{-(5-6)}$ over the wavelength range of 800–2000 nm was revealed using the time-dependent Schrodinger equation (TDSE) and the strong field approximation calculations [11–15]. More recently the first experimental measurement [16] at the single-atom level showed that the wavelength scaling is $\lambda^{-6.3\pm1.1}$ in Xe and $\lambda^{-6.5\pm1.1}$ in Kr over the wavelength range of 800–1850 nm. In addition, the wavelength dependence was found not smooth on a fine λ scale, but exhibiting fluctuations due to

*Electronic address: zhinan_zeng@mail.siom.ac.cn
†Electronic address: ruxinli@mail.shcnc.ac.cn
‡Electronic address: zzxu@mail.shcnc.ac.cn

 © 2014 THE PHYSICAL SOCIETY OF THE REPUBLIC OF CHINA

quantum-path interference [12–14]. The change of wavelength scaling with the ionization potential for single atom response was observed by M. V. Frolov *et al.* [13] for the first time. Popmintchev *et al.* [9] confirmed this behavior in a large ensemble of atoms and under phase matching conditions. Furthermore, Ref. [15] reported that the harmonic yield is nearly independent of the driving laser wavelength when the target atoms are irradiated simultaneously by an XUV pulse with the cut-off energy and ionization yield fixed.

So far, the reported wavelength scaling λ^x of HHG yield was obtained mainly for several typical target atoms, i.e. He, Ar, Xe and Kr. The yield of the high harmonics can be simply written as $|\langle\Psi_0|\,\bar{r}\,|\Psi_c\rangle|^2$, where Ψ_0 is the fundamental state of the atom and Ψ_c is the return electron (continuum state). For the return electron wavepacket, the Ψ_0 looks like a δ function. For longer wavelength pulse, the return electron wavepacket will expand much larger and reduce the harmonic yield as λ^{-3}. Also, longer wavelength will increase the photon energy as λ^2. That means if we sum the harmonic yield within the frequency region of ΔE, the ΔE will also increase as λ^2 when the laser wavelength is increased. But in previous work, the ΔE is kept constant. So the summed harmonic yield will decrease as λ^{-2}. Then, it can be understood that λ^{-3} is from the spread of the ionized wavepacket and λ^{-2} arises from the U_p quadratically increasing with λ. It is not understood where the factor in addition to λ^{-5} comes from and why the power x varies for different atoms. In this work, we theoretically investigate the dependence of the HHG yield on λ using atoms of different ionization potentials. It is found that the power x of the wavelength scaling λ^x surprisingly oscillates in the region $-3.63 \sim -6.32$ when the ionization potential is varied. A similar oscillation is found in the wavelength scaling of ionization ratio upon the ionization potential, indicating that the wavelength scaling of HHG yield is closely relevant to the ionization.

We first numerically solve the 1D TDSE in the length gauge for a linearly polarized laser field, and the TDSE is treated in a single-active electron approximation (SAE) [17] with spin-orbit coupling neglected,

$$i\frac{\partial}{\partial t}\psi(z,t) = \left[-\frac{1}{2}\nabla^2 + V_{soft}(z) + z * E(t)\right]\psi(z,t) \tag{1}$$

where $E(t) = E_0 f(t)\sin(\omega t)$ denotes the laser electric field, with E_0 the peak amplitude and $f(t)$ the envelope. The atom is subjected to an 8-cycle flat-top laser pulse, which is switched "on" and "off" in a half cycle. The peak intensity of driving laser field is fixed at 1.6×10^{14} W/cm^2, and a variation of λ over a range of 800–2000 nm is adopted.

We employ the soft-core Coulomb potential $V = -1/\sqrt{x^2 + C}$ to describe the target atom, where C represents the softening parameter. In the calculations, we vary the softening parameter $C$from 0.8 to 1.4 by an interval $\Delta C = 0.005$, corresponding to a change in the ionization potential from -0.735 a.u. to -0.582 a.u., and study how the λ scaling of HHG yield changes with respect to the ionization potential. The harmonic spectrum is obtained from the direct Fourier transform of the dipole acceleration, and the integrated HHG yield is defined in a fixed energy interval from 20 – 50 eV. Fig. 1 shows that the power x of the wavelength scaling λ^x are -4.77, -4.86 and -5.13 for the ionization potential of -0.735 a.u., -0.670 a.u. and -0.621 a.u., respectively.

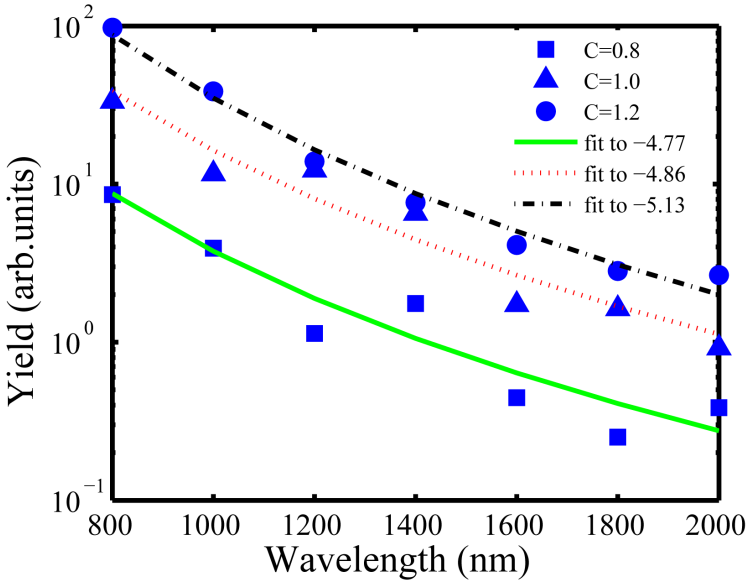

FIG. 1: The wavelength dependence of the integrated HHG yield (20–50 eV), obtained by using three different softening parameter $C = 0.8$ (■), 1.0 (▲) and 1.2 (•), corresponding to three different ionization potential $I_p = -0.735$ a.u., -0.670 a.u. and -0.621 a.u., respectively. The green solid line, red dashed line and black dot-dashed line show a $\lambda^{-4.77}$, $\lambda^{-4.86}$ and $\lambda^{-5.13}$ dependence, respectively.

One of the main results of this work is the evolution of power x of HHG yield upon the ionization potential, as shown in Fig. 2. A surprising oscillation of the power x around -5 can be seen. The maximum and minimum values of the power x are -3.63 at $Ip = -0.638$ a.u. and -6.32 at $Ip = -0.706$ a.u., respectively. When the ionization potential is deeper than -0.621 a.u., the separation of the adjacent peaks of the power x are $Ip_1 = 0.013$ a.u., $Ip_2 = 0.025$ a.u., $Ip_3 = 0.029$ a.u. and $Ip_4 = 0.032$ a.u., respectively. The oscillation of the power x slows down gradually with the decrease in the ionization potential, i.e., the period of the oscillation is becoming larger and larger. When the ionization potential proceeds less than -0.621 a.u., it is noticed that the ionization ratio (In our TDSE simulation, "ionization ratio" is defined as $P(t) = 1 - \|\psi(t)\|^2$, where $\psi(t)$ is the time-dependent wavefunction.) in the case of the 2000 nm is as high as 24%.

To analyze the remarkable phenomena shown in Fig. 2, we calculate the corresponding λ scaling of the ionization ratio upon the ionization potential. The ionization ratio as a function of the ionization potential for different λ from 800 to 2000 nm is shown in Fig. 3 (a). The λ scaling of the ionization ratio are presented in Fig. 3 (c), in which an oscillation similar to that shown in Fig. 2 can be seen. A detailed comparison of Fig. 3 (b) (reproduced from Fig. 2) and (c) tells us that two oscillation curves match each other very well, with every peaks (labeled by the red dashed lines) and valleys (labeled by the blue dashed lines) appearing at the same values of the ionization potential, until that the ionization potential is approaching -0.621 a.u. and beyond. The very low ionization potential leads to a large

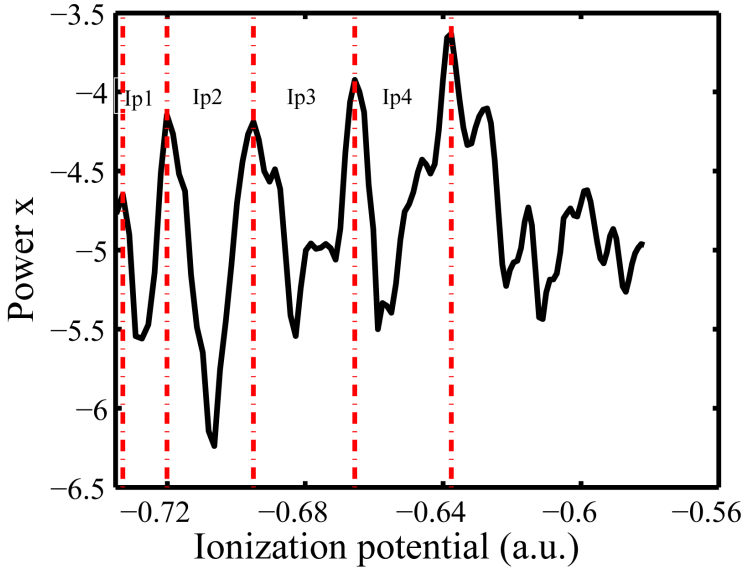

FIG. 2: The power x of wavelength scaling λ^x of the integrated HHG yield as a function of the ionization potential from -0.735 a.u. to -0.582 a.u.. $Ip_1 = 0.013$ a.u., $Ip_2 = 0.025$ a.u., $Ip_3 = 0.029$ a.u. and $Ip_4 = 0.032$ a.u. denote the interval of the adjacent peaks of the oscillation curve.

ionization ratio and the depletion of the ground state, the wavelength scaling law would therefore change considerably.

We also calculate the photoelectron spectra (PES) of different ionization potentials. The results obtained using the TDSE solved with the method of Ref. [18] for the 2000 nm pulse are shown in Fig. 4. One can see a complicated interference pattern. In the calculation, all the PES for different ionization potentials are from the absorbed wavefunction, which means that the integration of the PES of each ionization potential is the ionization ratio shown in Fig. 3 (a). As pointed out recently by H. R. Reiss [19], that the PES is affected by two factors, the momentum factor $F(p)$ and the generalized Bessel function $J_n(u, v)$, which lead to the complicated interference fringes. In the momentum factor, $p = n\omega - E_B - U_p$ and E_B is the ionization potential of the atom. We think that the complicated interference pattern in Fig. 4 can also be explained by these two factors. Because of the interference pattern shown in Fig. 4, the ionization ratio in Fig. 3 (a) for all the driving laser wavelengths do not increase monotonically with the ionization potential, with considerable fluctuations appearing in the evolution curves. Many peaks and valleys appear on the curves, but at different values of the ionization potential for different laser wavelengths.

Now we can explain the observed oscillation in the power x of the wavelength scaling λ^x of the ionization ratio and the HHG yield. If we define the scaling law represented by the smooth curves as "normal", the fluctuation of the curves will make the scaling law "abnormal". For example, if a peak appears at $Ip = -0.656$ a.u. for the 800 nm wavelength, but no peak showing up here for the 2000 nm wavelength, then the power x in the scaling

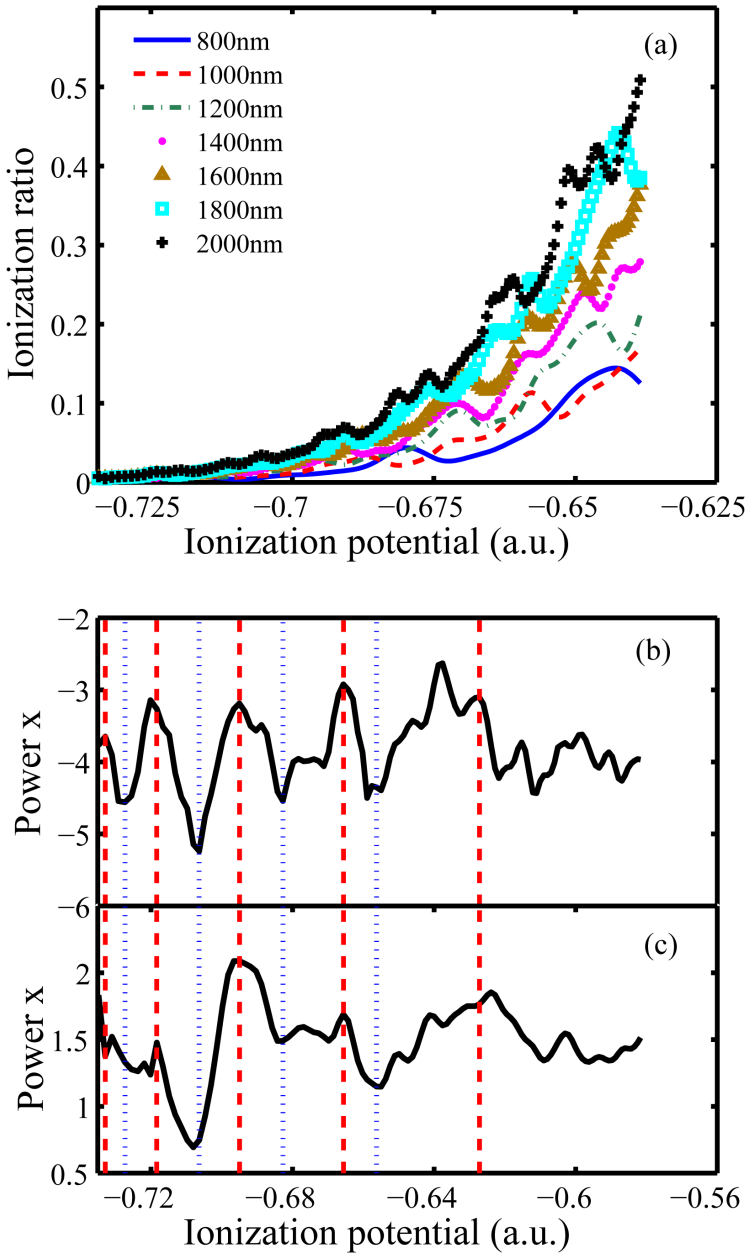

FIG. 3: (a) Ionization ratio as a function of the ionization potential for different laser wavelength from 800 nm to 2000 nm. (b) The same as Fig. 2. (c) The power x of the wavelength scaling λ^x of the ionization ratio as a function of the ionization potential. The red and blue dashed lines are used to label the peaks and valleys of the oscillation curves, showing a good matching in two scaling laws.

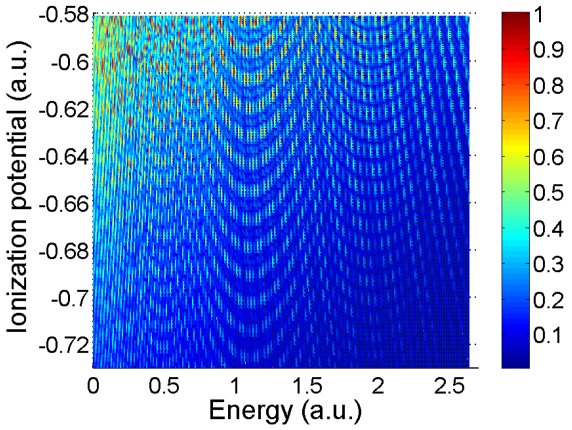

FIG. 4: The photoelectron energy spectrum as a function of the ionization potential, calculated by using the TDSE and a 2000 nm driving laser pulse. Complicated interference structures appear.

law will be smaller than the normal value. But if a peak appears at $Ip = -0.670$ a.u. for the 2000 nm wavelength, but no peak showing up there for the 800 nm wavelength, then the power x in the scaling law will be larger than the normal value. Consequently, the oscillation of the power x of the wavelength scaling λ^x appears.

Further investigation using a 3D TDSE is performed also. For the 3D model, we use the helium atom model [20] to do the calculation. The soft core model is written as [21]

$$V = -\frac{1}{r}\left(1 + e^{-2.505r}\right) \tag{2}$$

$$r = \sqrt{\rho^2 + z^2} + C \tag{3}$$

where ρ and z are radial and axial variables in the cylindrical coordinate.

The power x as a function of the ionization potential is shown in Fig. 5 (a). When the ionization potential is deep, e.g. -0.8 a.u., the center of the oscillation of the power x is about -6. With the decrease of the ionization potential, the center of oscillation moves to -5.5 gradually. This is similar to the results obtained with the 1D model that the center of the oscillation increases with the decrease of the ionization potential. When the ionization potential is around -0.5 a.u., the ionization ratio becomes larger and the power x begins to decrease. In comparison with the results of 1D model, the power x obtained by 3D TDSE is more sensitive to the change in the ionization potential. We speculate that two additional dimensions will induce more complex interference for the electron wavepacket. Fig. 5 (b) shows in more details a part of the curve for the atomic potential between -0.7 a.u. and -0.6 a.u. Although the fluctuation of the power x is more sensitive to the atomic potential in the 3D TDSE simulation, we can draw the same conclusion as that of the 1D TDSE simulation from Fig. 5 (b). Two curves match each other very well, with every peaks (labeled by the red dashed lines) and valleys (labeled by the blue dashed lines) appearing almost at the same values of the ionization potential.

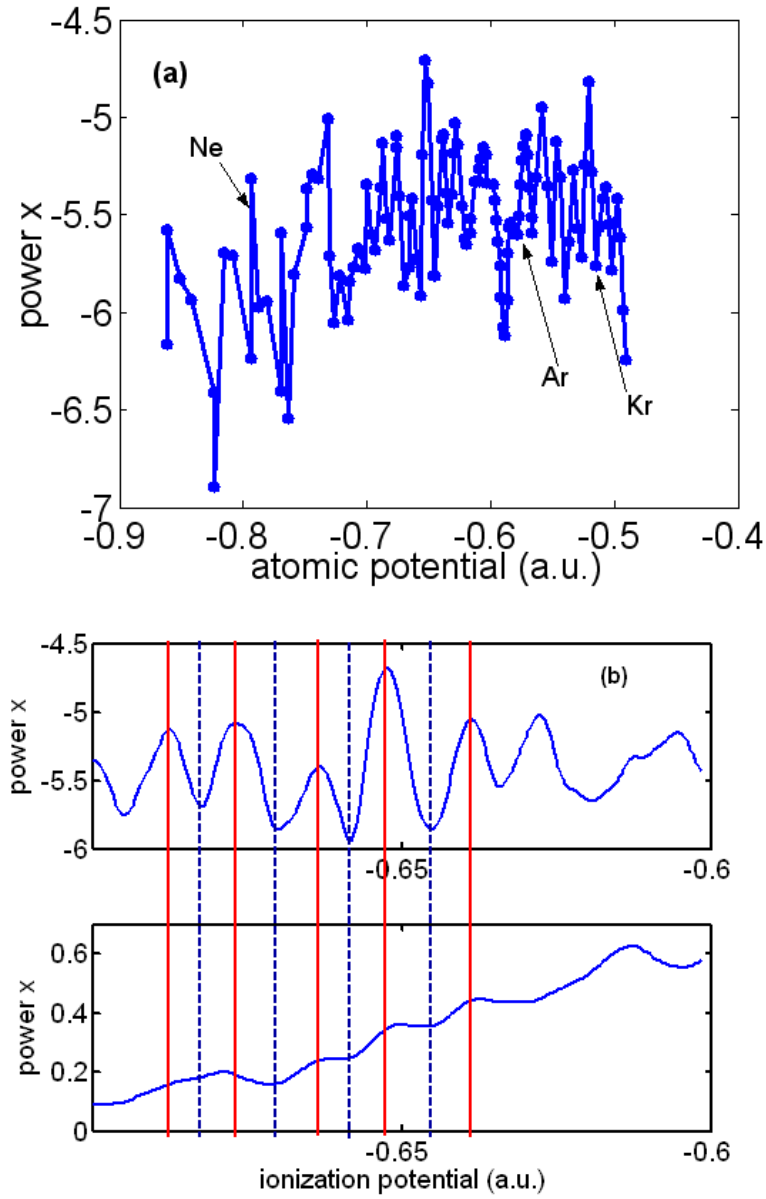

FIG. 5: (a) The power x of the wavelength scaling λ^x of the integrated HHG yield as a function of the ionization potential, obtained by using the 3D model. The ionization potential changes from -0.861 a.u. (close to He atom) to -0.490 a.u. (close to H atom). (b) Enlargement of (a) between -0.7 a.u. to -0.6 a.u.. The red and blue dashed lines are used to label the peaks and valleys of the oscillation curves.

The 3D TDSE calculation results for different noble gas are Ne (0.7928 a.u., $x = -5.4$), Ar (0.5794 a.u., $x = -5.6$), Kr (0.5147 a.u., $x = -5.8$), and Xe (0.4460 a.u., $x = -7.2$) , respectively. The laser intensity was assumed to be 1.6×10^{14} W/cm^2 except

that for Xe is 8×10^{13} W/cm^2. In the previous work, the power x are -5.5 for Ar (obtained theoretically) [12], -6.5 ± 1.1 for Kr (obtained experimentally at laser intensity of 1.3×10^{14} W/cm^2) and -6.3 ± 1.1 for Xe (obtained experimentally at laser intensity of 8×10^{13} W/cm^2) [16]. According to our calculations, if the laser intensity is 1.6×10^{14} W/cm^2, the power x will become larger when the atomic potential is smaller than 0.5 a.u. at which the ground state is depleted too much. Actually, the atomic potential has the discrete nature. It is difficult to observe experimentally and directly the oscillation of power x found in this work. But some effects due external fields may be used to test the prediction, e.g. Stark or Zeeman effects, due to which the energy level of the atom will shift.

We should point out that, based on the TDSE simulation, it is impossible to obtain the accurate value of the power x for each noble gas, because it is difficult to model a true atom accurately. For example, the power x reported in Ref. [12] for the hydrogen is -4.8, but the analytic result reported in Ref. [22] is -5.2. The difference in the absolute values of the power x reported in different works is related to the difference in the modeling. In this work, we do not attempt to obtain the accurate value of the power x for each noble gas, while we attempt to understand why the power x is so strange, e.g. it is not an integer as reported in previous works. By taking the effect of ionization into account, we can now understand where the factor in addition to λ^{-5} comes from and why the power x varies for different atoms in previous investigations. Ionization potential is found to play an important role in the wavelength scaling law. The curve of ionization ratio as a function of ionization potential is not a smooth one. For a special ionization potential, e.g. Ar or He, the power in the scaling law may be smaller or larger than the "normal" value.

In conclusion, the wavelength scaling of the HHG yield for atoms with different ionization potential has been investigated. It is found that the power x of wavelength scaling λ^x exhibits a surprising strong oscillation which slows down gradually with increasing ionization potential. We also explore the wavelength dependence of the ionization ratio as a function of ionization potential. It shows a remarkable oscillation similar to the wavelength scaling of the HHG yield, in which every peak and valley accurately match each other. The effect of ionization potential is also investigated with the 3D model. The oscillation of the power x is more sensitive to the change in the ionization potential. We think it can be attributed to the more pronounced electron wavepacket interference in the 3D model. However, the relationship among the ionization ratio and HHG yield scaling, and the ionization potential is still a subject need to be explored further. Furthermore, the single-active electron approximation is considered in the present work. If multiple electrons are considered, some additional effects may affect the wavelength scaling greatly, e.g. Cooper minima, electron correlation effects [22].

Acknowledgements

This work was supported by the National Natural Science Foundation of China (Grants No. 11127901, No. 61221064, No. 11134010, No. 11227902, No. 11222439, No. 11274325, and No. 61108012), the 973 Project (Grant No. 2011CB808103), and Shanghai

Commission of Science and Technology (Grant No. 12QA1403700). and Shanghai Supercomputer Center.

References

[1] J. L. Krause *et al.*, Phys. Rev. Lett. **68**, 3535-2528 (1992).
[2] K. C. Krause *et al.*, in Superintense Laser-Atom Physics, NATO Advanced Study Institute Series B: Physics, edited by B. Piraux *et al.*, (Plenum, New York, 1993), Vol. **316**, p. 95.
[3] W. Quan *et al.*, Phys. Rev. Lett. **103**, 093001 (2009).
[4] P. Colosimo *et al.*, Nat. Phys. **4**, 386-389 (2008).
[5] E. J. Takahashi *et al.*, Appl. Phys. Lett. **93**, 041111 (2008).
[6] T. Popmintchev *et al.*, Opt. Lett. **33**, 2128-2130 (2008).
[7] E. J. Takahashi *et al.*, Phys. Rev. Lett. **101**, 253901 (2008).
[8] M.-C. Chen *et al.*, Phys. Rev. Lett.**105**, 173901 (2010).
[9] T. Popmintchev *et al.*, Proc. Natl. Acad. Sci. U.S.A. **106**, 10516 (2009).
[10] M. Lewenstein *et al.*, Phys. Rev. A **49**, 2117-2132 (1994).
[11] J. Tate *et al.*, Phys. Rev. Lett. **98**, 013901 (2007).
[12] K. Schiessl *et al.*, Phys. Rev. Lett. **99**, 253903 (2007).
[13] M. V. Frolov *et al.*, Phys. Rev. Lett. **100**, 173001 (2008).
[14] K. L. Ishikawa *et al.*, Phys. Rev. A **79**, 033411 (2009).
[15] K. L. Ishikawa *et al.*, Phys. Rev. A **80**, 011807 (2009).
[16] A. D. Shiner *et al.*, Phys. Rev. Lett. **103**, 073902 (2009).
[17] K. C. Kulander, Phys. Rev. A **36**, 2726-2738 (1987).
[18] X. M. Tong *et al.*, Phys. Rev. A **74**, 031405 (2006).
[19] H. R. Reiss, Phys. Rev. Lett. **102**, 143003 (2009).
[20] E. J. Takahashi *et al.*, Phys. Rev. Lett. **99**, 053904 (2007).
[21] I. P. Christov *et al.*, Phys. Rev. Lett. **78**, 1251-1254 (1997).
[22] M. V. Frolov *et al.*, Phys. Rev. Lett. **102**, 243901 (2009).